LETTER Communicated by Odelia Schwartz

Neural Model of Coding Stimulus Orientation and Adaptation

Henrikas Vaitkevičius
henrikas.vaitkevicius@ff.vu.lt
Algimantas Švegžda
algimantas.svegzda@ff.vu.lt
Rytis Stanikūnas
rytis.stanikunas@ff.vu.lt
Remigijus Bliumas
remigijus.bliumas@fsf.vu.lt
Institute of Psychology, Vilnius University, LT-01513 Vilnius, Lithuania

Alvydas Šoliūnas
alvydas.soliunas@gf.vu.lt
Institute of Bioscience, Vilnius University, LT-10257 Vilnius, Lithuania

Janus J. Kulikowski
janus.kulikowski@manchester.ac.uk
Faculty of Biology, Medicine and Health, University of Manchester, Manchester M13 9PL, U.K.

The coding of line orientation in the visual system has been investigated extensively. During the prolonged viewing of a stimulus, the perceived orientation continuously changes (normalization effect). Also, the orientation of the adapting stimulus and the background stimuli influence the perceived orientation of the subsequently displayed stimulus: tilt aftereffect (TAE) or tilt illusion (TI). The neural mechanisms of these effects are not fully understood. The proposed model includes many local analyzers, each consisting of two sets of neurons. The first set has two independent cardinal detectors (CDs), whose responses depend on stimulus orientation. The second set has many orientation detectors (OD) tuned to different orientations of the stimulus. The ODs sum up the responses of the two CDs with respective weightings and output a preferred orientation depending on the ratio of CD responses. It is suggested that during prolonged viewing, the responses of the CDs decrease: the greater the excitation of the detector, the more rapid the decrease in its response. Thereby, the ratio of CD responses changes during the adaptation, causing the normalization effect and the TAE. The CDs of the different local analyzers laterally inhibit each other and cause the TI. We show that the properties of this model are consistent with both psychophysical and

https://doi.org/10.1162/neco_a_01269

neurophysiological findings related to the properties of orientation perception, and we investigate how these mechanisms can affect the orientation's sensitivity.

1 Introduction

Coding of sensory information has been studied both psychophysically and neurophysiologically. Contour orientation is the key feature for stimulus recognition. Orientation perception and its effects have been studied psychophysically for some time. It has been shown that the perceived orientation of stimuli depends on both the history of stimulus displaying (adaptation) and the background pattern (Gibson, 1933; Köhler & Wallach, 1944; Gibson & Radner, 1937; Held, 1963; Morant & Harris, 1965; Ganz, 1966; Blakemore, Carpenter, & Georgeson, 1970; Campbell & Maffei, 1971; Mitchell & Muir, 1976). Various perceptual effects have been identified. During adaptation or the prolonged viewing of the same stimulus, its perceived orientation continuously changes—a normalization effect (Gibson, 1933; Gibson & Radner, 1937). The orientation of preceded stimulus affects the perception of the followed stimulus and gives rise to the illusion of tilt after-effect (TAE). The background pattern affects the perceived orientation of stimulus and it gives rise to the tilt illusion (TI). (See Table 1.)

However, only in the middle of the previous century were electrophysiological correlates of stimulus perception established (Barlow, 1953; Hubel & Wiesel, 1959; Levick, 1967). The researchers found the neurons, so-called orientation detectors (OD), which fire selectively for different orientations of the stimulus. The responses of these neurons depend on the history of the stimulus being displayed (Müller, Metha, Krauskopf, & Lennie, 1999; Bednar & Miikkulainen, 2000; Dragoi, Sharma, & Sur, 2000; Dragoi, Sharma, Miller, & Sur, 2002; Sur, Schummers & Dragoi, 2002; Felsen, Shen, et al., 2002; Jin, Dragoi, Sun, & Seung, 2005; Gutnisky & Dragoi, 2008; Ghisovan, Nemri, Shumikhina, & Molotchnikoff, 2009) and on the visual patterns where the stimulus is being displayed (Blakemore & Tobin, 1972; Dragoi & Sur, 2000; Wissig & Kohn, 2012). However, it is not yet clear what neural adaptation mechanisms are responsible for the changes in the perception of line orientation. It is natural that most authors assume that the perception depends on the responses of a set of ODs—in other words, on a distributed presentation of responses (Lehky & Sejnowski, 1990; Schwartz, Sejnowski, & Dayan 2009). As the parameters of this distribution are crucial for the perception, it is important to know what these parameters are, how they arise, and how stimuli modify them.

Several models have been put forward to address these problems. The first model is based on experimental data, which show that the number of detectors tuned to vertical or horizontal lines are greater than those tuned to oblique orientations, that is, the anisotropic distribution of orientation

Table 1: List of Acronyms and Terms.

Term	Description
Adapter	The long-observed stimulus that precedes a test stimulus.
Attraction	The test stimulus is perceived as rotated toward an adapter or inducer.
Cardinal detector (CD)	The formal neuron broadly tuned to an orientation that forms a set of linearly independent detectors (i.e., the responses of which are not correlated).
Cardinal vector (CV)	The 2D vector formed from responses of two independent CDs.
Global analyzer	The set of neurons processing signals from a set of local analyzers.
Inducer	The observed stimulus displayed next to the test stimulus.
Local analyzer	The set of neurons directly receiving signals from a small, local part of retina
Orientation detector (OD)	The formal neuron narrowly tuned to a specific orientation and receiving signals from two CDs. The responses of ODs are correlated.
Orientational sensitivity	Described by the just noticed differences of stimulus orientations.
Preferred orientation	The orientation of stimulus that arouses the maximum response of a given OD.
Receptive field (RF)	The part of the retina that transmits signals to a local analyzer.
Repulsion	The test stimulus is perceived as rotated away from the adapter or inducer.
Tilt aftereffect (TAE)	The perceived orientation of the preceding stimulus affects the perceived orientation of the following stimulus.
Tilt illusion (TI)	The perceived orientation of a line is changed by the presence of surrounding lines of different orientations

detectors (Campbell & Kulikowski, 1966; King-Smith & Kulikowski, 1981; Li, Peterson, & Freeman, 2003). This model also suggests that the distribution of responses across the set of ODs determines the perceived line orientation. Both the adaptation and the background pattern change this distribution of responses across the set of OD. Thus, the TAE and TI stem from the changes of the distribution of OD responses. The characteristics of the TAE and normalization effect depend on the particular characteristics of the distribution (Clifford, Wederoth & Spehar, 2000; Storrs & Arnold, 2015; Schwartz, Sejnowski, & Dayan 2009; Bednar & Miikkulainen, 2000; Dragoi et al., 2000; Dragoi, Rivadulla, & Sur, 2001; Ghisovan et al., 2009; Priebe, 2016; Mayo & Smith, 2017). Unfortunately, we do not yet completely understand how the adaptation and the background pattern modify the distribution of responses over the set of the ODs according to this approach. Clifford (2014) proposed a modified distributed representation, where the

orientational sensitivity of the pool of orientation detectors is modified by inhibitory signals transmitted to the inputs of the cortical neurons. However, neither the source nor the control mechanism of inhibition signals are known, so it is difficult to estimate the quantitative properties of these models and, consequently, difficult to compare the predictions of such models with the real experimental data.

Another problem is that the relationship between neuron responses (neurophysiological data) and perception of the stimulus orientation (psychophysical data) is still not clear (Ghisovan et al., 2009). Not only is it unclear which neurons are affected by adaptation but also how adaptation and TI modify the distribution of the responses over the set of ODs. Some models suggest that the adaptation shift of the preferred orientation could emerge "from a recurrently connected network without plasticity" (Quiroga, Morris, & Krekelberg, 2016; see also Mayo & Smith, 2017). According to these models, inertia (persistence of a response after offset of a stimulus) causes the preceding adapter and the following test stimulus to overlap in time. As a result of this overlapping, a shift of the preferred orientation of the ODs occurs. The authors conclude, "This demonstrates that, in a recurrent network, adaptation on time-scales of hundreds of milliseconds does not require plasticity" (Quiroga et al., 2016, 58). However, these models fail to explain the influence of an adapter on longer adaptation.

On the basis of psychophysical findings, Held (1963), Templeton, Howard, and Easting (1965), and Wenderoth and Zwan (1989) suggested that the influence of an adapter on the perception of an orientation of a following test stimulus depends on two factors: one is perceptual figural, which depends on the interaction among nonlocal parts of image and produces TI, and the other is local, which produces TAE. Morant and Harris (1965) also wrote that the perceptual TAE is the result of the joint impact of two processes. Templeton et al. (1965), after careful investigation of the possible impact of these two processes on orientation perception, also concluded that both mechanisms could operate together.

To explain the noted factors, the two-stage model was proposed by Vaitkevičius, Karalius, Meškauskas, Sinius, and Sokolov (1983) and Vaitkevičius et al. (2009). According to this model, two sets of the orientation-sensitive neurons exist. The first has a small number of independent neurons broadly tuned to the orientation of the stimulus. The second consists of a large number of neurons, which are narrowly tuned to the different orientations of the stimulus. These neurons sum up with the given weighting the output responses of the neurons of the first set. This model can qualitatively estimate how the adaptation and the processes related to the TI have an impact on the responses of orientation detectors and the perception of orientation of stimuli (Vaitkevičius et al., 2009). However, the quantitative properties of the model were not investigated (i.e., the relationship between neuron responses and perception of the stimulus orientation was not analyzed).

The aim of this letter is to reconstruct and expand on the mentioned model (Vaitkevičius et al., 2009) and to then use this model to determine quantitatively the influence of the adaptation and processes related to the TI on both the responses of orientation detectors and the perception of stimulus orientation. Two responses of CDs determine cardinal vector (CV) in 2D Cartesian coordinate space. The proposed Cartesian coordinates differ from those used in other models (Clifford et al., 2000; Kuhlmann & Vidyasagar, 2011). The preferred orientation of the given OD is uniquely determined by the orientation of the CV. The greater is the response of the CD, the faster it decreases during adaptation. The TI stems from lateral inhibition among the CDs excited by the test stimulus and the inducer. Thus, knowing the distribution of OD responses, we can calculate how adaptation and TI affect the perception of orientation.

The analysis of CDs and ODs responses reveals that the adaptation differently changes their response gain (i.e., response magnitude) and orientational sensitivity. The adaptation reduces the response gain of the CDs but does not change the orientation selectivity. However, the adaptation maximally reduces the response gain of ODs tuned to cardinal orientation of the stimulus and affects the orientational selectivity of all ODs. If the adapter is vertical, with a horizontal or diagonal line oriented at 45°, the orientational sensitivity of ODs does not change. When the adapter is oriented at 22.5°, 67.5°, and 112.5°, it maximally affects the orientational sensitivity of ODs. Adaptation maximally improves orientation sensitivity of the set of ODs when the adapter is similar or largely dissimilar with respect to the test orientation (compare with the findings of Gutnisky & Dragoi, 2008). It should be noted that if the orientational sensitivity increases in one range of angles, then it inevitably decreases in another range, and on average, across the whole range of orientations, it does not change.

2 Structure of Formalized Model of Orientation Selectivity

The basic elements of our model (see Figure 1A) are formal neurons, which algebraically sums up the input signals. A stimulus is mapped in a small region (receptive filed, RF) of the local analyzer. Orientation (φ) of this stimulus is coded by the responses $\{x_1(\varphi), x_2(\varphi)\}$ of two independent cardinal detectors (CDs) that form the 2D vector ($\vec{E}(\varphi) = \{x_1(\varphi), x_2(\varphi)\}$ cardinal vector, CV). Orientation of this vector uniquely codes the orientation of the local stimulus. Besides the CDs, there are many orientation detectors (ODs), that combine to calculate the orientation of the stimulus (Vaitkevičius et al. 2009). The maximally excited OD determines the orientation of the stimulus. During prolonged exposure of an adapter, the CD responses decrease: the more excited the CD, the more its response decreases in a process of local adaptation. As the stimuli usually excite the CDs to a different extent, the orientation of the CV changes during adaptation.

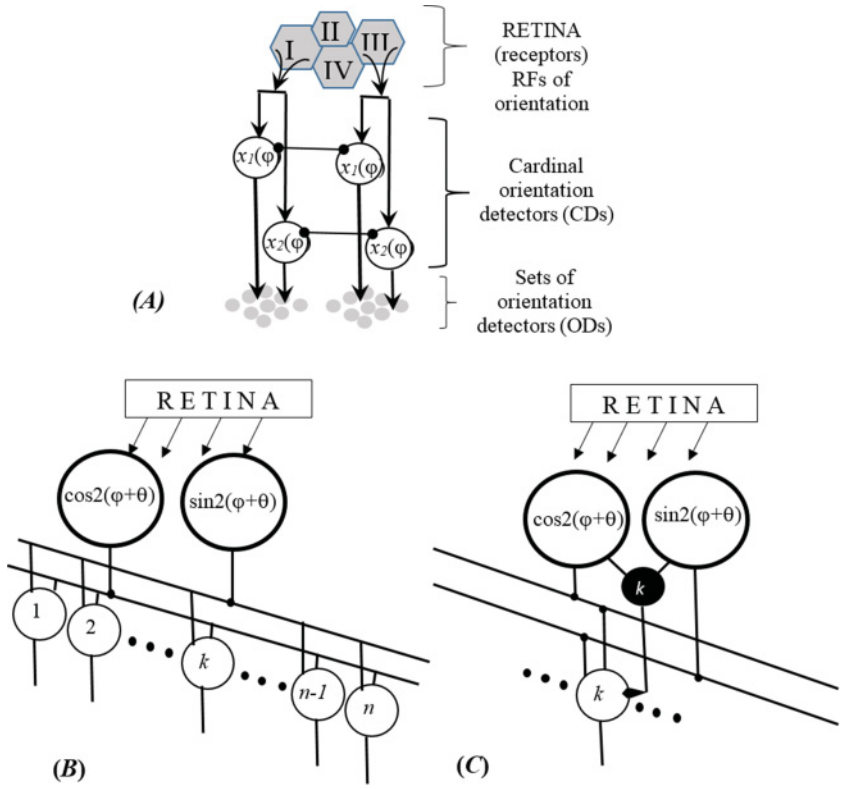

Figure 1: Model of the orientation analyzer. (A) I, II, . . . , IV. Two cardinal detectors (CDs) ($x_1(\varphi)$, $x_2(\varphi)$) sum up signals of receptors located in the RF of the local analyzer; they are broadly tuned to the orientations of stimuli. Orientation detectors (ODs) are tuned to different stimulus orientations. These detectors sum up signals of CDs with given weightings. These two CDs and a set of ODs, which obtain signals from these CDs, compose a local analyzer of orientation. The same kinds of CDs of different local analyzers inhibit each other. (B) Two-layer and (C) three-layer models of a local analyzer. The signals from the RF are transmitted to the inputs of two CDs, the orientation selectivity of which is described by functions $\cos2(\varphi + \theta)$ and $\sin2(\varphi + \theta)$. The output signals of CDs are transmitted to the inputs of neurons marked by numbered circles $(1, \ldots, k, \ldots, n-1, n)$. These orientation-selective neurons sum up the signals of CDs with the given weightings. White circles represent the orientation-selective neurons. Black circles represent neurons generating inhibitory signals, which inhibit orientation-selective neurons (white circle). In a three-layer model, an activated inhibitory neuron quenches the output response of OD (Whitmire & Stanley, 2016).

Furthermore, there are many local analyzers in the visual system, and each has its own two CDs and a set of ODs. The same types of CDs across the different local analyzers mutually inhibit each other (lateral inhibition in the orientation domain). The processes of the different analyzers overlap in time due to inertia produced by an adapter, and the local stimulus and nonlocal test stimulus jointly affect the responses (see Figure 10 in appendix A). Thus, the adaptation responses of the ODs stem from the joint actions of these local and nonlocal processes.

2.1 Construction of Orientation Selective Detectors (ODs). The local orientation analyzer gets signals from receptors located in an RF of the analyzer. The dependencies of the output responses of the CDs are described by the two following functions:

$$x_1(\varphi) = \cos 2(\varphi + \theta) \quad \text{and} \quad x_2(\varphi) = \sin 2(\varphi + \theta), \tag{2.1}$$

where θ stands for phase, which equals 22.5° (Vaitkevičius et al., 1983; Vidyasagar, 1985; Foster & Ward, 1991a, 1991b). The two signals of the CDs form the components of a two-dimensional vector $\vec{E}(\varphi)$. Changing angle φ from 0° to 180°, causes vector $\vec{E}(\varphi)$ to change its orientation from 0° to 360° (see Figure 2; the solid black circles denote the end of vectors).

The OD sums up the weighted output signals of the CDs (see Figures 1B and 1C). The output signal of the kth OD $z_k(\varphi)$ could be calculated by

$$\begin{aligned} z_k(\varphi) = c_{k1}x_1(\varphi) + c_{k2}x_2(\varphi) &= \left(\vec{C}_k(\varphi_k), \vec{E}(\varphi)\right) \\ &= \left|\vec{C}_k(\varphi_k)\right| \left|\vec{E}(\varphi)\right| \cos(\widehat{\vec{C}_k, \vec{E}}). \end{aligned} \tag{2.2}$$

The weightings of the two connections of the kth OD will be denoted by $\{c_{k1}, c_{k2}\}$ $(k = 1, \ldots, n)$. They form the two-dimensional connection vector $\vec{C}_k(\varphi_k)$ of the kth OD. Assume that the magnitude of this vector is constant: $|\vec{C}_k(\varphi_k)| =$ constant. Each OD is tuned to a different stimulus orientation, that is, each one maximally sensitive to a given line orientation. So that the response of the kth OD will be at its maximum under exposure of the given line orientation φ_k, the connection vector $\vec{C}_k(\varphi_k)$ should be collinear with the given vector $\vec{E}(\varphi_k)$ (Fomin, Sokolov, & Vaitkevicius, 1979). Hence, the orientation of vector $\vec{E}(\varphi_k)$ uniquely codes the orientation of the line: the kth OD is maximally excited relative to others, when vectors $\vec{E}(\varphi_k)$ and $\vec{C}_k(\varphi_k)$ are collinear.

It should also be noted that according to the experimental results (Sillito, 1975; Ferster & Koch, 1987; Worgotter & Koch, 1991; Ben-Yishai, Bar-Or & Sompolinsky, 1995; Sompolinsky & Shapley, 1997), the orientation selectivity of the detectors vanishes or is significantly reduced when the inhibition signals are suppressed. That is difficult to explain with the two-layer

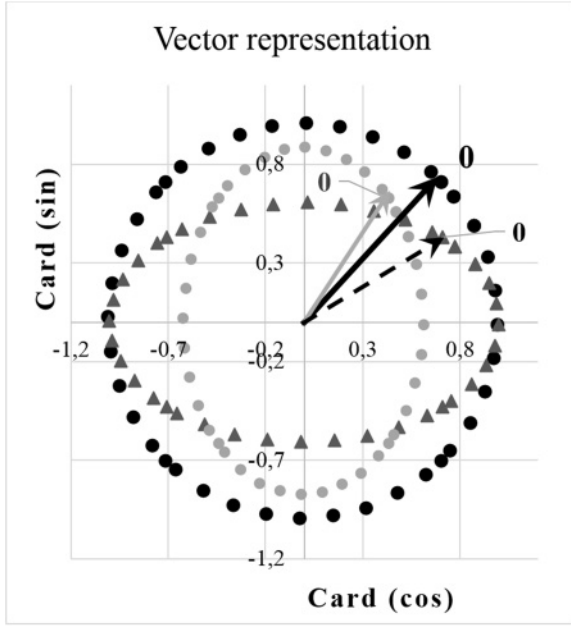

Figure 2: Vector coding of line orientations. Responses of the cosine CD are on the abscissas; on the ordinate are responses of the sine cardinal one. The black circles represent the end of vectors corresponding to the lines of different orientations ($0^\circ \leq \varphi < 180^\circ$) in the absence of an adaptation. The black triangles and gray circles represent vectors corresponding to the same physical lines displayed after the adapter oriented at 22.5° and at 60°, respectively. The solid black vectors oriented at 45° represent the vertical line preceding the adapter. The gray and dashed vectors represent the physical vertical line after adaptation to lines oriented at 60° and 22.5°, respectively.

model (see Figure 1B). In order to take into account the neurophysiological findings, the two-layer model could be transformed into a three-layer model (see Figure 1C). It is suggested that each neuron (black circle) inhibits the response of the output OD (white circle). An output neuron is active if the response of the inhibitory neuron equals zero. Let us assume that the kth inhibitory neuron also sums up the weighted signals provided by the CDs. Assume that the connection weightings of the inhibitory neuron also form the components of two-dimensional vectors $\vec{C}_k^+(\varphi_k)$ orthogonal to vector $\vec{E}(\varphi_k)$.

Hence, the kth OD will generate its maximal signal when vector $\vec{E}(\varphi_k)$ is collinear to the connection vector of this neuron and orthogonal to the connection vector $C_k^+(\varphi_k)$ of the inhibitory neuron. Thus, this model codes

the orientation of the vector under which the output response of the kth inhibitory neuron equals zero. The structure of the three-layer model is consistent with the neurophysiological findings of Whitmire and Stanley (2016; see Figure 5), who showed that sensory excitatory input to a cortical neuron is usually accompanied by inhibitory input through an intermediate neuron.

2.2 Adaptation in the Local Analyzer: Local Adaptation. Let us assume that the changes of the CD orientational sensitivity during prolonged viewing depend on both the orientation of adapter (angle φ_a) and duration time (t):

$$x_j(\varphi/\varphi_a, t) = x_j(\varphi)\exp(-\gamma(t)|x_j(\varphi_a)|), (j = 1, 2). \tag{2.3}$$

That could be presented in vector notation:

$$\vec{E}(\varphi/\varphi_a, t) = A(\varphi_a t)\vec{E}(\varphi), \tag{2.3a}$$

where A(φ_a, t) stands for the operator of the adaptation; $x_j(\varphi/\varphi_a, t)$ stands for the jth CD response to the line of the given orientation (φ), which is displayed after the adapter; and $\gamma(t)$ is a function of adaptation time t (Greenlee & Magnussen, 1987; Bednar & Miikkulainen, 2000; Dragoi et al., 2000).

Responses ($z(\varphi/\varphi_a, t)$) of the kth OD as function (φ, φ_a, t) can be calculated in the following way:

$$z_k(\varphi/\varphi_a, t) = c_{k1}x_1(\varphi/\varphi_a, t) + c_{k2}x_2(\varphi/\varphi_a, t) = (\vec{C}_k(\varphi_k)\vec{E}(\varphi/\varphi_a, t)). \tag{2.4}$$

2.3 Interaction among Local Analyzers. Many local analyzers are involved in analyzing the orientation of a stimulus image displayed on the RF of a local analyzer. After removing a stimulus from the receptive field, its effect does not vanish immediately, and it interacts with later stimuli in this receptive field, modifying the perception of orientation (Sekuler & Littlejohn, 1974; Vaitkevicius et al., 2009). This is the TAE, a local adaptation mechanism. It is well documented that along with the local adaptation, there are nonlocal mechanisms that change the perceived orientation of the test stimulus (Song et al., 2013; Müller, Schillinger, Do, & Leopold, 2009). These mechanisms are related to increasing differences in orientation (orientation contrast) between different lines, simultaneously displayed (Blakemore et al., 1970; Blakemore & Tobin, 1972; Sekuler & Littlejohn, 1974; Dragoi & Sur, 2000; Müller et al., 2009). The TAE and the orientation simultaneous contrast (or TI), as functions of line orientations, are described by Blakemore and Tobin (1972), Wenderoth and Zwan (1989), Jin et al. (2005), and Müller et al., 2009.

Let us assume that on two RFs of different local analyzers (the lth and sth analyzers), two different lines oriented at φ and $\varphi + \Delta$ are displayed, respectively. The interaction between these local neighbor analyzers could be described in the following way:

$$\vec{E}_l'(\varphi, \Delta) = \vec{E}_l(\varphi) - \alpha \vec{E}_s(\varphi + \Delta). \tag{2.5}$$

Vector $\vec{E}_l'(\varphi, \Delta)$ is generated by the lth local system taking into account the influence of the signal ($\vec{E}_s(\varphi + \Delta)$) generated by neighbor sth local system. This expression means that there is lateral inhibition between the same type of CDs of the lth and sth local systems; the strength of inhibition is described by the coefficient $0 < \alpha < 1$.

Taking into account the mutual lateral inhibition between CDs of local analyzers, the response of the lth OD as a function of the angle Δ between two lines could be calculated in this way:

$$\begin{aligned} z_l(\varphi, \Delta) = (\vec{C}_l(\varphi), \vec{E}_l'(\varphi + \Delta)) &= (\vec{C}_l(\varphi)\left(\vec{E}_l(\varphi) - \alpha \vec{E}_s(\varphi + \Delta)\right) \\ &= 1 - \alpha \cos 2\Delta. \end{aligned} \tag{2.6}$$

As we see, the responses of the given detector depend only on the difference Δ in orientations between two lines.

3 Comparisons of Model Properties with the Existing Psychophysical Data

The TAE and TI depend mainly on the transformation of responses of the two CDs already described.

3.1 Influence of Adaptation on the Responses of the CDs and Perception of Test Stimulus. The maximally excited OD in a set of ODs determines the perceived orientation of the stimulus. With an analysis of the influence of adaptation and a simultaneous orientation contrast on an orientation of cardinal vectors (CVs), we can determine how these processes influence the orientation selectivity of ODs and determine TAE and the process of normalization in the network.

Vector presentation related to coding stimulus orientation is shown in Figure 2, where solid circles and gray circles, triangles mark the ends of vector $\vec{E}(\varphi)$, representing a stimulus oriented at the given angle φ before and after adaptation. Responses of cosine and sine CDs are on the abscissa and ordinate axes, respectively. How the adapter changes the CD responses and thereby the CV orientation is clearly shown in Figure 3.

Taking into account that $\theta = 22.5^\circ$, the vertical line (solid black, $\varphi = 0^\circ$) before adaptation should activate both CDs equally (the cosine

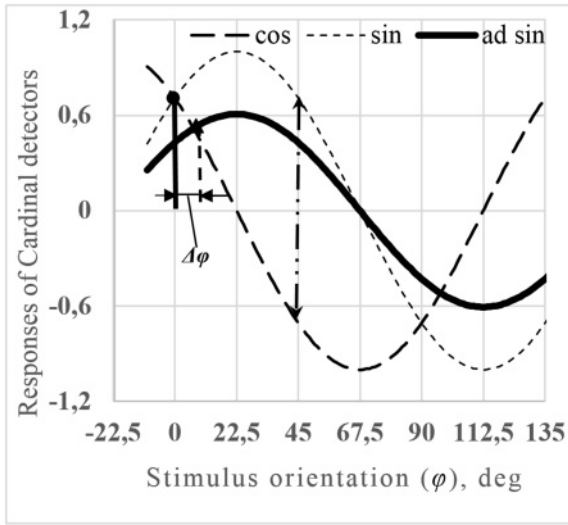

Figure 3: Orientational sensitivities of two CDs as functions of stimulus orientation before and after adaptation to line oriented by 22.5°. Abscissa: orientation of stimulus φ in degrees (orientation of vertical line equal 0°). Ordinate: CD responses. The dashed line describes the sensitivity of the cosine detector before and after adaptation. The thin dashed line and solid line present the sensitivity of sine detector before and after adaptation respectively.

(dashed) and sine (thin dashed) detectors), $x_1(\varphi) = x_2(\varphi) = \cos 2(22.5^\circ) = \sin 2(22.5^\circ)$. In other words, the point where both lines intersect determines the responses of two CDs to a vertical line. The situation changes after adaptation to a line oriented at 22.5°. In this case, the adapter activates the sine- but does not activate cosine CD (see Figure 3). Hence, during the adaptation, only the response gain of the sine detector decreases; the response gain of the nonactivated cosine detector does not change. As a result, the vertical line ($\varphi = 0^\circ$), after adaptation activates these CDs unevenly. New responses of CDs as a function φ are presented by the dashed and solid black curves. The solid black vertical line appears to be turned counterclockwise relative to the "perceived" vertical line (see Figure 3, short dashed vertical); the true vertical, that is, appears to be turned counterclockwise relative to the "perceived" vertical (repulsion effect, TAE). If the adapter is oriented at -22.5°, it activates the cosine and does not activate the sine CD. In this case, we again have a repulsion effect: TAE.

3.2 Different Influences of Adaptation on the Magnitude of Responses of the CDs and ODs. According to equations 2.3, 2.3a, and 2.4, the responses of the cardinal and orientation detectors depend on the

adaptation. However, the influence of the adapter on the CD and OD responses differs significantly. The magnitude of CD responses during prolonged exposure to an adapter decreases independently over the whole interval of angle φ (see equation 2.3). However, at the same time, their orientational sensitivities are not changed.

The influence of the adaptation on the OD responses is more complicated. The responses depend on both the magnitude of the vector, (see equation 2.3 a) $\vec{E}(\varphi/\varphi_a, t)$ and its orientation, equation (2.4). Because the adapter changes the orientation and magnitude of vector $\vec{E}(\varphi/\varphi_a, t)$, the preferred orientation and magnitude responses of ODs also change. This corresponds to neurophysiological findings obtained by Dhruv and Carandini (2014) that an adaptation reduces the response gain of CDs but does not change their preferred orientation; however, the adaptation changes both the response gain of ODs and their preferred orientations.

First, taking into account the adaptation, the magnitude of the OD response to the preferred orientation at φ_k can be calculated from the following bilinear form (slightly modified from equation 2.4):

$$z_k(\varphi/\varphi_k, t) = (A(\varphi_k/\varphi_k, t)\vec{E}_k(\varphi_k); \vec{E}(\varphi_k)).$$

The value of this bilinear form is minimal for the eigenvector. Hence, the responses of ODs tuned to either horizontal or vertical lines decrease maximally during adaptation. Unfortunately, this prediction was not checked experimentally. To test this prediction, the time course of adaptation should be simultaneously recorded for orientation-selective neurons with different preferred orientations.

Second, the changes of the preferred orientation of ODs also stem from the changes of the orientation of vector $\vec{E}(\varphi/\varphi_a, t)$.

3.3 Influence of Adaptation on the Orientation Selectivity of ODs. If the adaptation mechanism already described has a place in the brain, it should arouse the changes in the orientation selectivity of ODs (see Figure 4).

Indeed, considering neurophysiological data, some authors have shown that if the angle between an adapter and test stimuli is in the range 0° to 30°, the preferred orientations of detectors are shifted away from the adapting stimuli, whereas when angle $\Delta\theta$ was in the range 45° to 67.5°, the shift of the preferred direction changes, but an adapter oriented at the cardinal orientations does not shift the test stimuli (Bednar & Miikkulainen, 2000; Dragoi et al., 2000 (see their Figure 1F); Felsen et al., 2002; Müller et al., 1999). The average maximal shift was observed when the angle between an adapter and test stimuli ($\Delta\theta$) was equal to about 22.5° (Dragoi et al., 2000, Figure 1E). The properties of ODs of our model are qualitatively in agreement with the experimental data.

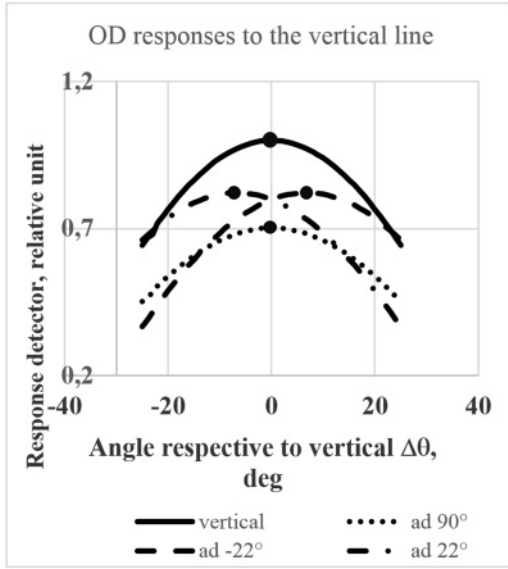

Figure 4: Influence of adaptation on responses of the model OD. Calculated responses of the vertical line detector before and after adaptation to $\pm 22.5^\circ$ and 90° (see the legend) versus test line orientation φ. Responses to stimuli preceding the adapter are presented by a solid black line.

The responses of the ODs, the preferred orientation of which equals 0° (a vertical line) as a function of angle φ in the model before and after adaptation, are pictured in Figure 4. The solid curve represents the OD responses before adaptation. The dotted, dash-dotted, and dashed curves represent the responses to stimuli oriented at 90° (or 0°) and $\pm 22.5^\circ$, respectively, after adaptation. The horizontal (or vertical) adapter changes the magnitude of responses but not the orientation selectivity of the OD. The adapters oriented at $\pm 22.5^\circ$ cause a repulsive shift of the vertical test stimulus. These properties of the model are consistent with the experimental data. Calculating the relationships, we assume that the CD responses after adaptation decrease by 20% from their initial responses. The shift of the preferred orientation of the given OD is the same in both two- and three-layer models.

The adapter can initiate not only repulsion but also attraction. The sets of the CVs modified by the adapter oriented at 22.5° and 60° are shown by triangles and gray circles, respectively (see Figure 2). The ends of the CVs of the true vertical stimulus before and after adaptation to the adapter oriented at 22.5° and 60° are represented by black circles, triangles, and gray circles, respectively. While the angle between the vertical line and adapter

is smaller than $\pm 45^\circ$, the repulsion effect occurs, and for greater angles, the attraction effect occurs.

Moreover, it should be noted, in an experimental situation, the OD responses depend on two processes: local and nonlocal ones (Held, 1963; Templeton et al., 1965; Wenderoth & Zwan, 1989; Dragoi & Sur, 2000; Jin et al., 2005; Müller et al., 2009; Song et al., 2013). The joint impact of both of these neural mechanisms on the tilt illusion of test stimulus observed after adaptation is discussed below.

3.4 Influence of Adaptation on Perceived Orientation. Let us assume that a perceived line orientation depends on the preferred orientation of the maximally excited OD. In order to compare the properties of the model with the known experimental data, we simulated the same psychophysical experiments using the proposed model.

Initially, the dependence of the responses of the detector with a given preferred orientation was determined as a function of orientation φ. Let us assume that this detector is maximally sensitive to a vertical line ($\varphi = 0$), referred to below as the test line. After that, an adapter oriented at $\Delta\theta$ angle relative to the test line was exposed for a long time. After adaptation, the response of the same neuron as a function of φ was again determined. The aim was to determine how the adapter changes the responses of OD as a function of the angle $\Delta\theta$ between the adapter and test stimulus.

3.4.1 Adaptation and Perceptual TAE. Let us assume that the real orientation of the test line is φ. After exposure to an adapter oriented at φ_a, vector $\vec{E}(\varphi)$ is transformed to $\vec{E}(\varphi/\varphi_a, t)$. Angle $\Delta\Psi(\varphi/\varphi_a)$ between these two vectors determines the shift of the preferred orientation of the given detector. These functions versus angle ($\Delta = \varphi - \varphi_a$) were calculated for vertical, horizontal, and diagonal (oriented at 45°) lines and compared with analogical functions registered in experiments with humans.

The experimental and calculated TAE as a function of the adapter orientation φ_a are pictured in Figure 5. In a Morant and Harris (1965) study, a tilted line was observed for 1 min, and after a 7.5 s interval, the test line, horizontal or vertical, was presented. The subject had to adjust the test line to apparent vertical (or horizontal) orientation. The peak of TAE was observed at $+10^\circ$ from the vertical (see Figure 5A), and at about $+60^\circ$, the repulsion effect changed to attraction. In Campbell and Maffei (1971), an oblique grating was observed for 20 s. Then the orientation of a test grating was reported by rotating a stick (placed at one side of the test grating) until it appeared parallel with the vertical test grating. The peak of TAE was observed at $\pm 15^\circ$ from the vertical and disappeared exponentially at higher angles (see Figure 5B). In Müller at al. (2009), an adapter was slowly rotated during a 6 s period and after a sound signal while the line stimulus was stationary; the subject was required to report whether the stimulus rotated clockwise or counterclockwise. They found that an adaptation effect peak was at $\pm 15^\circ$

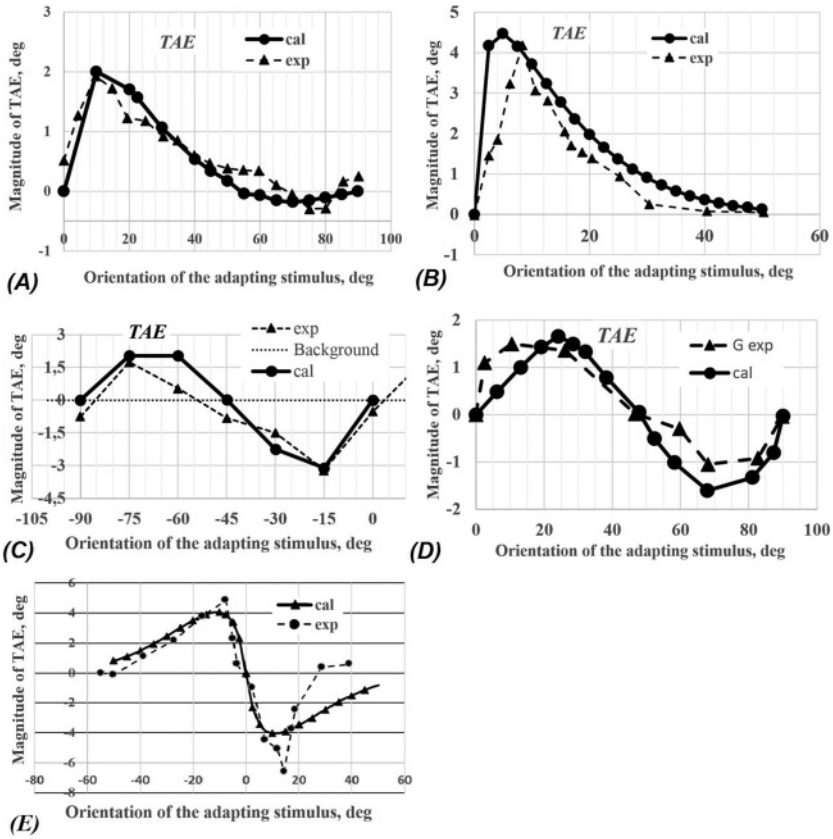

Figure 5: TAE as function of the adapter orientation. Experimental data described by Morant and Harris (1965) (A), Campbell and Maffei (1971) (B), Müller et al. (2009) (C), Gibson and Radner (1937) (D), Mitchell and Muir (1976) (E) are marked by solid circles, and calculated model simulations are marked by triangles.

and at $\pm 75^\circ$ (corresponding to $\pm 15^\circ$ from the horizontal stimulus) from the vertical stimulus (see Figure 5C). In Gibson and Radner (1937), a line tilted 5° from the vertical or horizontal was observed for 90 s. After a 2 min rest interval, the subject adjusted by hand the disc with the presented vertical (or horizontal) line during an 8 s interval until it appeared vertical (or horizontal). The authors found both effects—the repulsion and the attraction. The peak of repulsion effect was at about $+10^\circ$, and the peak of attraction was at about $+70^\circ$ (see Figure 5D). The TAE changed the direction at the $+45^\circ$ of adaptation line. In Mitchell and Muir (1976), an adapting grating was observed for 3 min. Then the test grating was presented for 2 s during

which the subject indicated its apparent orientation by rotating a luminous line situated 3° to the right of the test grating. The TAE peaks were observed at about +15° and −10° of adopting grating relative to a horizontal test grating. As seen in Figure 5, our model data match the data of psychophysical experiments quite well.

As indicated, the authors obtained different experimental data. Despite these differences, they can be described in our model by the same function, changing only two constants. One of them describes the speed of adaptation and influences mainly the magnitude of TAE. The other determines the magnitude of the lateral inhibition among the local orientation analyzers and changes the extremal point, where TI function is maximal (see appendix A).

3.4.2 Dynamic OD Responses during Adaptation: The Normalization Effect. During the prolonged exposure of noncardinal lines, their perceived orientation changes smoothly, a process known as the *normalization effect* (Gibson, 1933; Gibson & Radner, 1937; Köhler & Wallach, 1944; Greenlee & Magnussen, 1987). How can we explain the normalization effect with the proposed model?

Moreover, the orientational sensitivity of ODs tuned to vertical and horizontal lines does not change during adaptation (i.e., the preferred orientations of these detectors do not change). Adaptation is described by expression 2.3 or 2.3a: $\vec{E}(\varphi/\varphi_a, t) = A(\varphi_a, t)\vec{E}(\varphi)$.

Because adaptation does not change the perception of cardinal stimuli, it does not change the orientation of cardinal vectors representing the vertical and horizontal lines. In other words, these vectors are the eigenvectors of the adaptation operator $A(\varphi_a t)$. In our case, this operator has two pairs of eigenvectors, which should satisfy the following requirements:

$$\left|\cos 2(\varphi_a + 22.5^\circ)\right| = \left|\sin 2(\varphi_a + 22.5^\circ)\right|, (\varphi_a = 0, 45^\circ, 90^\circ, 135^\circ), \quad (3.1)$$

$$\left|\cos 2(\varphi_a + 22.5^\circ)\right| = 0 \; or \; \left|\sin 2(\varphi_a + 22.5^\circ)\right| = 0,$$
$$(\varphi_a = \pm 22.5^\circ, 67.5^\circ, 112.5^\circ). \quad (3.2)$$

Expression (3.1) represents vertical, horizontal, and oblique lines oriented at 45° and 135°, and expression (3.2) represents oblique lines oriented at ±22.5°, 67.5°, and 112.5°, lines located among lines in expression (3.1). The requirements of expression (3.1) mean that if stimuli excite both CDs equally, then during adaptation, the CVs do not change. The same occurs if stimuli excite only one CD, expression 3.2.

Detailed analysis shows that the lines of equation 3.2 are not stable, and any fluctuation in their orientations should produce their subjective rotation toward the nearest stable lines of equation 3.1 (Fomin, Sokolov, & Vaitkevicius, 1979). Unfortunately, we were able to find only one

publication in which these properties of lines in equation 3.2 were checked in detail experimentally (Vaitkevičius et al., 2009). However, there is insufficient information relating to the normalization effect of the diagonal lines oriented at 45° and 135°.

Mitchell and Muir (1976, 365) showed that "TAE occurs in the oblique meridian (stimulus oriented at 45°)". Moreover, the dependence of this effect as a function of angle $\Delta\theta$ between the diagonal and adapter is very similar to the corresponding relationships for the vertical and horizontal lines. It should be noted that according to these authors, there is no shift (TAE) when angle $\Delta\theta$ is equal to zero; the orientation of a line oriented at 45° does not change after prolonged viewing of the same oriented line (there is no normalization effect). This fact is consistent with the prediction of the model.

Let us consider this process in more detail. Assume that the adapter excites both CDs, but one of them (e.g., sine CD) is more excited than the other (cosine CD). According to equation 2.3, the output response of the more excited sine CD decreases faster than cosine CD. Hence, during adaptation, the CV produced by the stimulus is continuously rotating toward the nearest eigenvector; the maximum of responses over the set of ODs is thus shifting toward the OD tuned to cardinal orientation (see equation 3.1). As soon as that occurs, the adaptation changes in orientation of the CV stop. In other words, the distribution of the CVs within the interval 0° to 180° is changed, and these changes depend on the orientation of the adapter. However, after the adaptation, the cardinal vectors (eigenvectors) corresponding to the subjective vertical and horizontal lines will not change orientation in relation to each other, although the absolute orientations of physical lines that activate both CDs equally will change. This statement could be not valid for other vectors.

3.5 Influence of Interaction among Local Analyzer on the TI and OD Responses.

3.5.1 Influence on the TI. Along with the adaptation, the nonlocal lateral interactions among the CDs of the different local analyzers also affect both the perceived orientation of test stimulus and the responses of CDs and ODs. If the other line (inducer stimulus) is displayed in the in vicinity of the test line, then the perceived orientation of the test line changes depending on the angle (Δ) between the test and inducer lines (Blakemore et al., 1970; Müller et al., 2009). The repulsion effect is observed for acute angles, and the attraction is observed for obtuse angles higher than 90° (see Figure 12 in appendix B).

The experimental results of these authors are pictured in Figure 6. The interaction between test and inducer lines in the model using algorithms described in section 2.3 was also calculated (see equation 2.5 and appendix A).

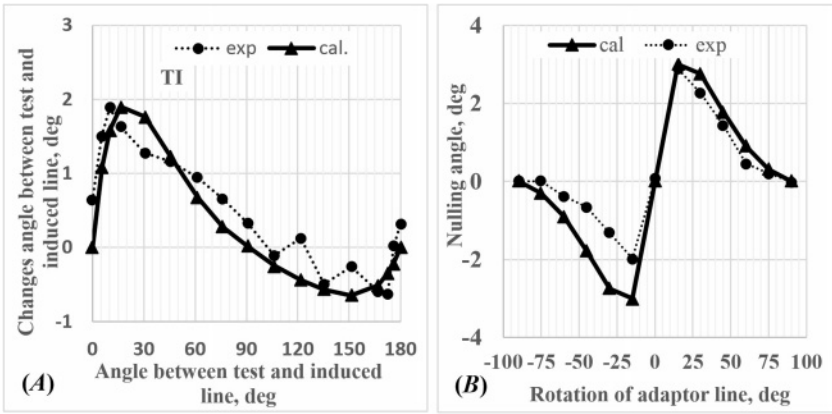

Figure 6: Tilt illusion as a function of orientation angle Δ between test and induced stimuli. The angle Δ between the inducer and test line is on the abscissa; changes of the perceived orientation of test line are on the ordinate. Solid black circles in both panels are the experimental data (left panel: Blakemore et al., 1970; right panel: Müller et al., 2009). The calculated model simulations are presented by the solid line marked by triangles.

The calculated dependence versus angle (Δ) is also pictured in Figure 6 (see the solid black line).

3.5.2 Influence of the Inducer on the Responses of ODs. According to Blakemore and Tobin (1972), the inducer maximally inhibits the response of OD when its preferred orientation coincides with the orientation of the inducer. The experimentally registered responses of the OD as a function of an angle Δ between the test and the inducer lines (inducer stimuli) are pictured in Figure 7.

The dotted line represents the response of the given detector to the preferred line in the absence of interactions ($\alpha = 0$). The dashed line represents the responses of the detector to the preferred line when a coefficient α is fixed ($\alpha = 0.8$). Taking into account that the averaged distance between test and induction lines increases with increasing angle Δ,it is assumed that coefficient α decreases exponentially with angle Δ. The solid line represents detector responses when coefficient α exponentially decreases with angle Δ. The responses of a detector are maximally inhibited when the test and induction lines are collinear ($\Delta = 0$). When the angle between lines increases, the inhibitory effect decreases. An excitatory effect replaces the inhibitory one, when the angle becomes larger than 45°. A similar result was experimentally obtained by Blakemore & Tobin, 1972; see also Dragoi & Sur, 2000).

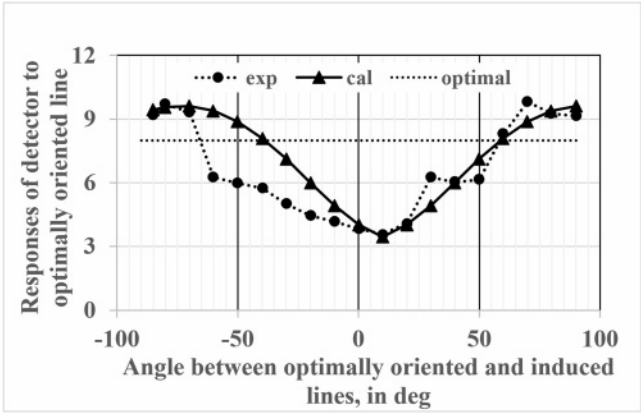

Figure 7: Responses of an OD as a function of angle Δ. Dotted lines with solid circles show the dependence of the responses of the detector to the preferred test line in the absence of and under the influence of the inducer respectively (Blakemore & Tobin, 1972). The solid line with solid triangles shows calculated model simulations.

4 Influence of Adaptation and Orientation Contrast on Orientational Sensitivity

Now the question arises as to how adaptation modifies the orientational sensitivity of the network. Let us assume that the sensitivity of the network is determined by the minimal angle ($\Delta\varphi$) of the line rotation, at which the maximum detector response is shifted from one detector to the nearest detectors. For the sake of simplicity, we assume that the ODs are homogeneously distributed over the angle interval (0°–180°). In this case the just-noticed line rotation ($\Delta\varphi$) could be determined by the just-noticed angle ($\Delta\Psi = 2\Delta\varphi$) between two vectors $\vec{E}(\varphi)$ and $\vec{E}(\varphi + \Delta\varphi)$. Before adaptation, the angle $\Delta\Psi =$ constant (see Figure 2). After adaptation the distribution of vectors changes. In some intervals, density decreases (angle between two neighboring vectors increases), but in other intervals, density increases (the angles decrease; see the gray circles and triangles). Thus, the sensitivity increases in the regions where angles between neighboring vectors are larger (a small rotation of the line produced the large angle in vector space and vice versa). However, increasing the resolution for some vectors means that the length of the circle arc, on which these stimuli are mapped, is stretched. But as the length of the whole circle is fixed, the enlargement of one part causes the shrinking of other parts. On average, the orientational sensitivity over the whole interval of angles should be constant.

In order to illustrate this statement we calculate the angles $\Psi(\varphi, \Delta) = \vec{E}(\varphi) - \vec{E}(\varphi + \Delta)$ and $\Psi(\varphi/\varphi_a, \Delta) = \vec{E}(\varphi/\varphi_a, t) - \vec{E}((\varphi + \Delta)/\varphi_a, t)$ as a

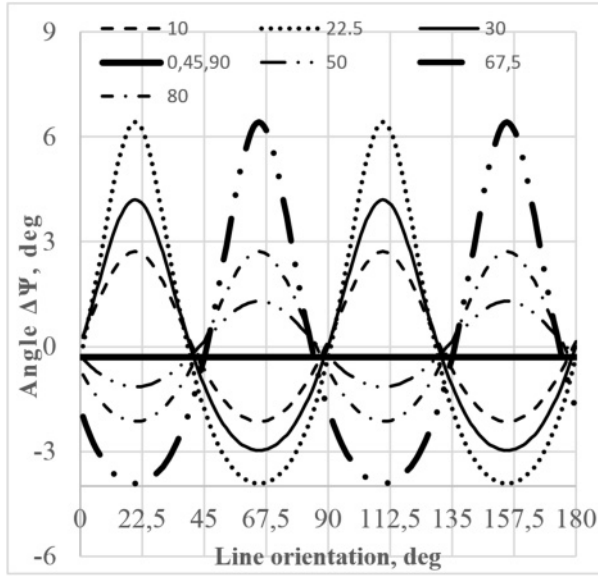

Figure 8: Impact of adaptation on the network orientational sensitivity. On the abscissa is a line orientation φ in degrees. On the ordinate, the difference ($\Delta\Psi$) in estimation of line orientation physically turned by 5°.

function of test line φ and adapter φ_a orientation before and after adaptation. Changes of sensitivity could be estimated by the following function: $\Delta\Psi(\varphi) = \Psi(\varphi/\varphi_a, \Delta) - \Psi(\varphi, \Delta)$. If $\Delta\Psi(\varphi)$ is positive, the sensitivity increases; it decreases when $\Delta\Psi < 0$. The results of these calculations are shown in Figure 8. Numbers in legends identify the orientation of the adapter in respect of the physical vertical line.

As seen, the adaptation to the vertical, horizontal, and diagonal lines oriented at 45° does not affect the orientational sensitivity of the network. The adapter located between these cardinal orientations affects orientational sensitivity significantly. Where differences in orientation of test lines and adapter do not exceed 45°, orientational sensitivity increases: $\Delta\Psi > 0$. Otherwise orientational sensitivity decreases: $\Delta\Psi < 0$. The increase of orientational sensitivity is maximal if both adapter and test lines are oriented at 22.5°, 67.5°, 112.5° or 157.5°. It should be noted that the average value of $\Delta\Psi$ always equals zero. Unfortunately, we could not find any experimental research addressing this problem. However, Gutnisky and Dragoi (2008, 220), studying the influence of adaptation on the responses of an OD population (neurons of V1 monkey cortex), wrote: "Post-adaptation changes in noise correlations cause the largest improvement in network performance

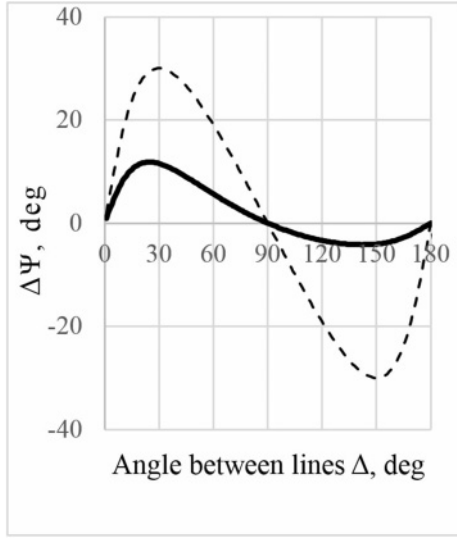

Figure 9: Impact of inhibitory interaction among local systems on the estimation of the physical angle between two lines. On the abscissa, the given angle between two lines, in degrees. On the ordinate, the differences of angles between physical and estimated angles, in degrees. Dashed line: lateral inhibition between two systems does not depend on angle α. Solid black line: the lateral inhibitory coefficient α exponentially decreases as physical angle Δ increases.

when test stimuli are similar or largely dissimilar with respect to the adapting orientation." The impact of adaptation on the orientational sensitivity of the population of ODs of our model is similar (see Figure 8).

In turn, orientation contrast or TI also regulates the orientational sensitivity of the model. In order to illustrate this statement, we calculated how TI subjectively changes the angles between two CD vectors $\vec{E}_l(\varphi)$ and $\vec{E}_s(\varphi + \Delta)$ corresponding to lines l and s oriented at angle φ and $\varphi + \Delta$, respectively. The differences between the given physical angle and the calculated one ($\Delta\Psi = \Psi(\alpha, \Delta) - \Delta$) as a function of physical angle Δ are pictured in Figure 9.

$\Psi(\alpha, \Delta)$ is a function of strength of interaction α and angle Δ. The dashed line is a function where coefficient α is constant ($\alpha = 0.5$); the solid black line was calculated when $\alpha = 0.5\exp(-f(\Delta))$. The greater coefficient α ($0 < \alpha < 1$) is, the greater is the maximum of the function, and its maximum is shifted more toward small angles Δ. The obtained results do not conflict with well-known experimental findings (Blakemore & Tobin, 1972; Dragoi & Sur, 2000; Jin et al., 2005).

5 Conclusion

1. The proposed model of a local analyzer explains the coding of line orientation. It consists of two independent CDs and many ODs. There are many local analyzers, the receptive fields of which are located in different areas of the retina.

2. The stimuli displayed in the receptive field of a local analyzer excite the two CDs, whose signals, with some weightings, are summed up linearly by ODs. The summed weightings of each OD are chosen in such a way that the preferred orientation of the given detector should depend on the ratio of CD signals uniquely. The vertical and horizontal lines excite both CDs equally.

3. During prolonged exposure to a stimulus, the output signals of CDs decrease, but their orientational sensitivities do not change. Although the connections among CDs and ODs do not change, the preferred orientations of ODs change.

4. The normalization effect and tilt aftereffect are results of adaptation. During the normalization process, the ratio of output signals of two CDs changes until they become equal.

5. If angles between test stimuli and adapter are less than about 60°, stimuli are repulsed from the adapter. If this angle is greater than 60°, the perceived test stimuli are attracted to the adapter. During this process, the orientational sensitivity increases in some regions while in others it decreases; however, on average, the orientational sensitivity does not change.

6. Along with the local tilt aftereffect, there is another process related to nonlocal interactions among different local analyzers. As a result of this interaction, the ability to discriminate the differences in orientations of stimuli increase (orientation contrast increases).

7. The observed adaptation effects stem from two processes: local adaptation (TAE) and nonlocal process (TI or orientation contrast).

In our opinion, the basic principles of the proposed model are not unique to orientation selectivity. They could be adapted to coding of visual stimulus movement and of stimulus location in 3D space (binocular analyzer) and expanded to the perception of tactile stimuli.

Appendix A: Joint Influence of Adaptation and Orientation Contrast on Determination of Line Orientation in the Model

Figure 10 presents the joint influence of adaptation and orientation contrast in physical space of local analyzers.

First, the adapter is exposed and oriented at angle φ_{ad}, which affects the CDs of a local analyzer. Second, after adaptation, the physical vertical test line oriented at angle $\varphi_v = 0$ is displayed, and the test line should be matched to a "subjective" vertical line. Hence, taking into account the

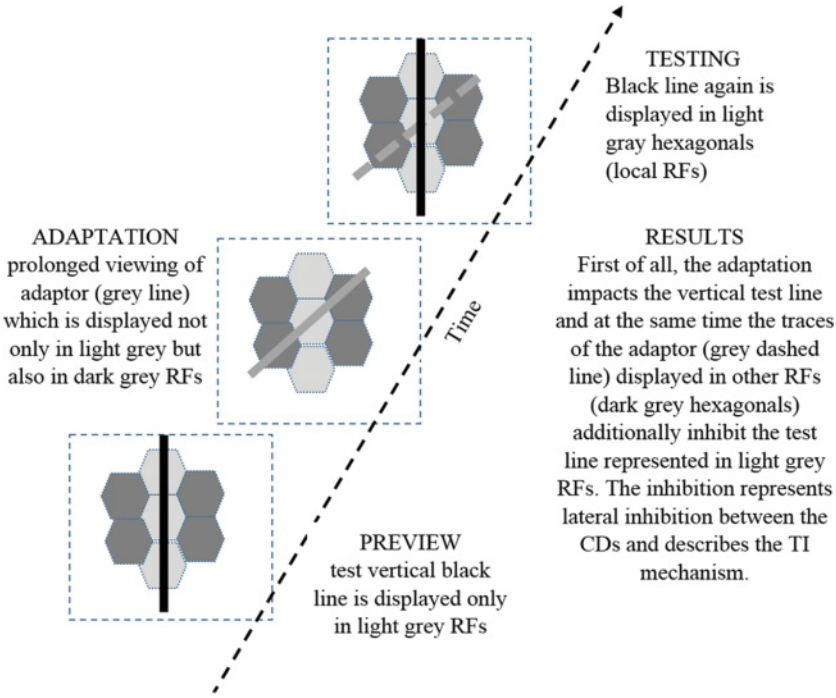

Figure 10: The joint influence of adaptation and orientation contrast on perception of the vertical test line. The test line is displayed first (Preview box), followed by the adapter (Adaptation box), and test line (Testing box). The results of the sequence of events are described in the Results box.

above, we have two interacted stimuli. After adaptation, the vertical line in the local analyzer corresponds to the vector $\vec{E}(\varphi_v/\varphi_{ad}) = A(\varphi_{ad}, t)\vec{E}(\varphi_v))$, and in the other neighboring analyzer, the trace of the adapting stimulus (inducer) corresponds to the vector $\mathrm{A}(\varphi_{\mathrm{ad}}, t)\vec{E}(\varphi_{\mathrm{ad}})$.

As results of the joint impact of these two stimuli on the CDs of the local analyzer, we have a new stimulus described by the following vector:

$$\vec{E}^{/}(\varphi_v/\varphi_{ad}) = A(\varphi_{ad}, t)[\vec{E}(\varphi_v) - \alpha\vec{E}(\varphi_{ad})]. \tag{A.1}$$

Without a nonlocal interaction, the influence of adaptation on the subjective changes of orientation of the test (vertical) in the local analyzer (i.e., TAE) is described by the angles

$$\Delta\psi_{ad} = \vec{E}(\varphi_v/\widehat{\varphi_{ad}}), \vec{E}(\varphi_v) = A(\varphi_{ad}, t)\widehat{\vec{E}(\varphi_v)}, E(\varphi_v).$$

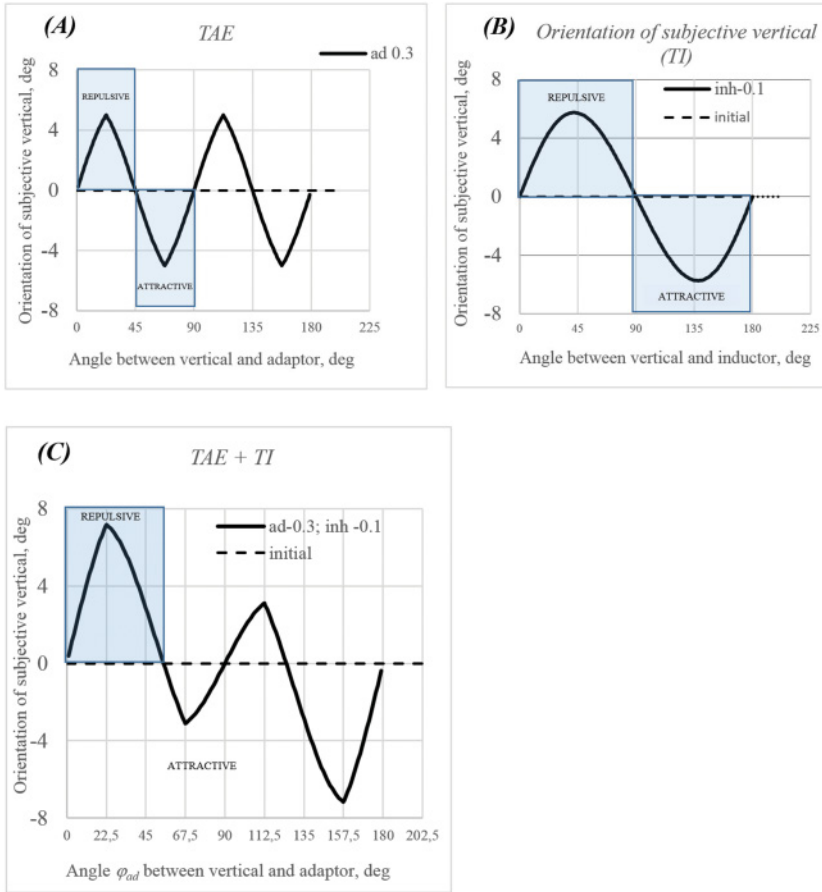

Figure 11: Orientation illusions stem from adaptation and simultaneous contrast (TI). On the abscissa is the angle (deg) between the test line and either the adapter or inducer. On the ordinate is an orientation of the vertical (test) line. (A) Changes of orientation (deg) of subjective vertical line versus the angle between the vertical (test) line and adapter. (B) Changes of orientation (deg) of subjective vertical line versus the angle between the vertical (test) line and inducer. (C) Changes of perceived orientation, taking into account, both the action TAE and TI jointly (i.e., panels A and B).

This dependence as a function of the angle between the adapter and test stimulus is shown in Figure 11A.

The influence of nonlocal interactions between neighboring analyzers on the changes of perception of vertical line orientation is characterized by the angle between two vectors:

$$\Delta\psi_{contr} = \left(\left[\vec{E}_l(\varphi_v) - \alpha\widehat{\vec{E}_n(\varphi_{ad})}\right], \vec{E}(\varphi_v)\right).$$

The first one, $\vec{E}_l(\varphi_v)$, corresponds to the test stimulus displayed in the RF of the lth local analyzer. Another vector, $\vec{E}_l(\varphi_v) - \alpha\vec{E}_n(\varphi_{ad}) = \vec{E}_l^{/}(\varphi_v, \Delta)$ stems from interaction between nonlocal analyzers (see equation 2.5). Here $\vec{E}_l(\varphi_v)$ stands for the test stimulus displaying in the RF of the lth local analyzer. Vector $\vec{E}_n(\varphi_{ad})$ stands for the adapter preceding the test stimulus mapped in the RF of the neighbor analyzer. The quantity $\Delta = \varphi_{ad} - \varphi_v$ stands for the physical angle between the adapter and test (vertical) stimulus.

The angle $\Delta'\psi_{\text{contr}}$ as a function of φ_{ad} is shown in Figure 11B.

The influence of both adaptation and lateral interaction on the perceived orientation of the test (vertical) line could be calculated as

$$\Delta\Phi = (\widehat{\vec{E}(\varphi_v/\varphi_{ad})}, \vec{E}(\varphi_v)) = (A(\varphi_{ad}, t)\left[\vec{E}(\varphi_v) - \alpha\vec{E}(\varphi_{ad})\right]\vec{E}(\varphi_v)).$$

Angle $\Delta\Phi$ as a function of φ_{ad} is shown in Figure 11C.

The calculated dependences of the model do not contradict different experimental data (see Figure 5, 6, and 9). In all cases, we used the same formulas for calculations, changing only two coefficients. The first of them changes the speed of adaptation and a magnitude of TAE. The second changes the extreme points of TAE, as well as its magnitude.

Appendix B: Repulsion and Attraction Effects in Case of Tilt Illusion

For simplicity, we explore the interaction between two lines (the vertical line oriented at $\varphi = 0^\circ$ and an arbitrary one, called the inducer, oriented at φ_i). In Figure 12, two different situations are analyzed. The black and gray solid lines on the left side of the figure represent the test line and inducer, respectively. The dashed black line represents the perceived orientation of the test line. The black and gray solid vectors at the right side of the figure represent the test $E(\varphi_t)$ and inducer $E(\varphi_i)$, respectively. It should be noticed that the angles between the vectors are two times larger than the angles between physical lines (see expression 2.1). We propose that lateral inhibition among cardinal detectors separately coding the inducer and test line is described in the following way: $E(\varphi_t|\varphi_i) = E(\varphi_t) - \alpha E(\varphi_i)$ (this procedure is explained at the right side of figure). While the angles between the inducer and test line are in range $-90^\circ < \varphi < 90^\circ$, the vector $E(\varphi_t|\varphi_i)$ (black dashed vector) is rotated counterclockwise (repulsion effect). However, while the angles between the inducer and test line are in the range $90^\circ < \varphi < 180^\circ$ the vector $E(\varphi_t|\varphi_i)$ is rotated clockwise (attraction effect; bottom right of the figure). It means that acute angles between lines are enlarged and obtuse angles are reduced. In other words, this procedure diminishes the correlation between the responses of detectors representing orientations of lines

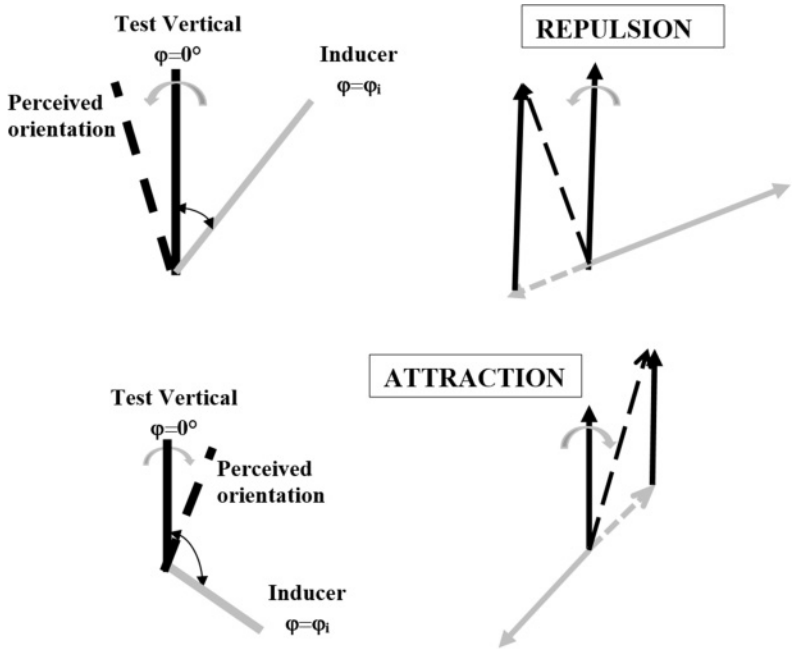

Figure 12: The principles of repulsion (top) and attraction (bottom). Physical positions of stimuli are presented on the left side, and the response vectors on the right side.

in a set of detectors and enlarges the ability to notice the differences in line orientations.

Acknowledgments

We thank the reviewers for their deep analysis and their remarks, which were extremely helpful in revising the manuscript. We also thank Jacqui Grant for help in preparing this letter.

References

Barlow, H. B. (1953). Summation and inhibition in the frog's retina. *J. Physiol.*, *119*, 69–88.

Bednar, J. A., & Miikkulainen, R. (2000). Tilt aftereffects in a self-organizing model of the primary visual cortex. *Neural Computation*, *12*(7), 1721–1740. https://www.mitpressjournals.org/doi/abs/10.1162/089976600300015321

Blakemore, C., Carpenter, R. H. S., & Georgeson, M. A. (1970). Lateral inhibition between orientation detectors in the human visual system. *Nature*, *228*(52662), 37–39. https://www.nature.com/articles/228037a0

Blakemore, C., & Tobin, E. A. (1972). Lateral inhibition between orientation detectors in the cat's visual cortex. *Experimental Brain Research*, *15*(4), 439–440. https://link.springer.com/article/10.1007%2FBF00234129

Ben-Yishai, R., Bar-Or R. L., & Sompolinsky, H. (1995). Theory of orientation tuning in visual cortex. *Proceedings of the National Academy of Sciences of the United States of America*, *92*(9), 3844–3848. https://doi.org/10.1073/pnas.92.9.3844

Campbell, F. W., & Kulikowski, J. J. (1966). Orientational selectivity of the human visual system. *Journal of Physiology*, *187*(2), 437–445. https://doi.org/10.1113/jphysiol.1966.sp008101

Campbell, F. W., & Maffei, L. (1971). The tilt after-effect: A fresh look. *Vision Research*, *11*(8), 833–840. https://doi.org/10.1016/0042-6989(71)90005-8

Clifford, C. W. G. (2014). The tilt illusion: Phenomenology and functional implications. *Vision Research 104*, 3–11. http://dx.doi.org/10.1016/j.visres.2014.06.009

Clifford, C. W., Wenderoth, P., & Spehar, B. (2000). A functional angle on some after-effects in cortical vision. *Proceedings of the Royal Society*, *267*(1454), 1705–1710. https://dx.doi.org/10.1098/rspb.2000.1198

Dhruv, N. T., & Carandini, M. (2014). Cascaded effects of spatial adaptation in the early visual system. *Neuron*, *81*(3), 529–535. https://doi.org/10.1016/j.neuron.2013.11.025

Dragoi, V., Rivadulla, C., & Sur, M. (2001). Foci of orientation plasticity in visual cortex. *Nature*, *411*(6833), 80–86. http://dx.doi.org/10.1038/35075070

Dragoi, V., Sharma, J., Miller, E. K., & Sur, M. (2002). Dynamic of neuronal sensitivity in visual cortex and local features discrimination. *Nature Neuroscience*, *5*(9), 883–891. http://dx.doi.org/10.1038/nn900

Dragoi, V., Sharma J., & Sur, M. (2000). Adaptation-induced plasticity of orientation tuning in adult visual cortex. *Neuron*, *28*(1), 287–298. https://doi.org/10.1016/S0896-6273(00)00103-3

Dragoi, V., & Sur, M. (2000). Dynamic properties of recurrent inhibition in primary visual cortex: Contrast and orientation dependence of contextual effects. *Journal of Neurophysiology*, *83*(2), 1019–1030. https://doi.org/10.1152/jn.2000.83.2.1019

Felsen, G., Shen, Y-S., Yao, H., Spor, G., Li, Ch., & Dan, Y. (2002). Dynamic modification of cortical orientation tuning mediated by recurrent connections. *Neuron*, *36*(5), 945–954. https://doi.org/10.1016/S0896-6273(02)01011-5

Ferster, D., & Koch, C. (1987). Neuronal connections underlying orientation selectivity in cat visual cortex. *Trends in Neurosciences*, *10*(12), 487–492. https://doi.org/10.1016/0166-2236(87)90126-3

Fomin, S. V., Sokolov, E. N., & Vaitkevicius, H. H. (1979). *Artificial sense organs*. Moscow: Nauka Press.

Foster, D. H., & Ward, P. A. (1991a). Asymmetries in oriented-line detection indicate two orthogonal filters in early vision. *Proceedings of the Royal Society B*, *243*(1306), 75–81. http://dx.doi.org/10.1098/rspb.1991.0013

Foster, D. H., & Ward, P. A. (1991b). Horizontal-vertical filters in early vision predict anomalous line-orientation identification frequencies. *Proceedings of Royal Society B*, *243*(1306), 83–86. http://dx.doi.org/10.1098/rspb.1991.0014

Ganz, L. (1966). Mechanism of the figural aftereffects. *Psychological Review*, *73*(2), 128–150. http://dx.doi.org/10.1037/h0022952

Ghisovan, N., Nemri, A., Shumikhina, S., & Molotchnikoff, S. (2009). Long adaptation reveals mostly attractive shifts of orientation tuning in cat primary visual cortex. *Neuroscience*, *164*(3), 1274–1283. http://dx.doi.org/10.1016/j.neuroscience.2009.09.003

Gibson, J. J. (1933). Adaptation, after-effect and contrast the perception of curved lines. *Journal of Experimental Psychology*, *16*(1), 1–31. http://dx.doi.org/10.1037/h0074626

Gibson, J. J., & Radner, M. (1937). Adaptation, after-effect and contrast in the perception of tilted lines. I Quantitative studies. *Journal of Experimental Psychology*, *20*(5), 453–467. http://dx.doi.org/10.1037/h0059826

Greenlee, M. W., & Magnussen, S. (1987). Saturation of the tilt aftereffect. *Vision Research*, *27*(6), 1041–1043. https://doi.org/10.1016/0042-6989(87)90017-4

Gutnisky, D. A., & Dragoi, V. (2008). Adaptive coding of visual information in neural populations. *Nature*, *452*(7184), 220–225. https://www.nature.com/articles/nature06563

Held, R. (1963). Localized normalization of tilted lines. *American Journal of Psychology*, *76*(1), 146–148. https://www.jstor.org/stable/1420015

Hubel, D. H., & Wiesel, T. N. (1959). Receptive fields of single neurons in the cat's striate cortex. *Journal of Physiology*, *148*(3), 574–591. http://dx.doi.org/10.1113/jphysiol.1959.sp006308

Jin, D. Z., Dragoi, V., Sur, M., & Seung, H. S. (2005). Tilt aftereffect and adaptation-induced changes in orientation tuning in visual cortex. *Journal of Neurophysiology*, *94*(6), 4038–4050. http://dx.doi.org/10.1152/jn.00571.2004

King-Smith, P. E., & Kulikowski, J. J. (1981). The detection and recognition of two lines. *Vision Research*, *21*(2), 235–250. https://doi.org/10.1016/0042-6989(81)90117-6

Köhler, W., & Wallach, H. (1944). Figural after-effects. An investigation of visual processes. *Proceedings of the American Philosophical Society*, *88*(4), 269–357. http://www.jstor.org/stable/985451

Kuhlmann, L., & Vidyasagar, T. (2011). A computational study of how orientation bias in the lateral geniculate nucleus can give rise to orientation selectivity in primary visual cortex. *Frontiers in Systems Neuroscience*, *5*, art. 81.

Lehky, S. R., & Sejnowski, T. J. (1990). Neural model of stereoacuity and depth interpolation based on a distributed representation of stereo disparity. *Journal of Neuroscience*, *10*(7), 2281–2299.

Levick, W. R. (1967). Receptive fields and trigger features of ganglion cells in the visual streak of the rabbit's retina. *Journal of Physiology*, *188*(3), 285–307. https://doi.org/10.1113/jphysiol.1967.sp008140

Li, B., Peterson, M. R., & Freeman, R. D. (2003). Oblique effect: A neural basis in the visual cortex. *Journal of Neurophysiology*, *90*(1), 204–217. http://dx.doi.org/10.1152/jn.00954.2002

Mayo, J. P., & Smith, M. A. (2017). Neuronal adaptation: Tired neurons or wired networks? *Trends in Neurosciences*, *40*(3), 127–128. https://doi.org/10.1016/j.tins.2016.12.001

Mitchell, D. E., & Muir, D. W. (1976). Does the tilt after-effect occur in the oblique meridian? *Vision Research*, *16*(6), 609–613. https://doi.org/10.1016/0042-6989(76)90007-9

Morant, R. B., & Harris, J. R. (1965). Two different after-effects of exposure to visual tilts. *American Journal of Psychology*, *78*(2), 218–226. https://www.jstor.org/stable/1420493

Müller, J. R., Metha, A. B., Krauskopf, J., & Lennie, P. (1999). Rapid adaptation in visual cortex to the structure of images. *Science*, *285*(5432), 1405–1408. http://dx.doi.org/10.1126/science.285.5432.1405

Müller, K.-M., Schillinger, F., Do, D. H., & Leopold, D. A. (2009). Dissociable perceptual effects of visual adaptation. *PLOS One*, *4*(7), e6183. https://doi.org/10.1371/journal.pone.0006183

Priebe, N. J. (2016). Mechanisms of orientation selectivity in the primary visual cortex. *Annual Reviews of Vision Science, 2*, 85–107. https://doi.org/10.1146/annurev-vision-111815-114456

Quiroga, M., Morris, A. P., & Krekelberg, B. (2016). Adaptation without plasticity. *Cell Reports*, *17*(1), 58–68. https://doi.org/10.1016/j.celrep.2016.08.089

Schwartz, O., Sejnowski, T. J., & Dayan, P. (2009). Perceptual organization in the tilt illusion. *Journal of Vision*, *9*(4), 1–20. https://jov.arvojournals.org/article.aspx?articleid=2193419

Sekuler, R., & Littlejohn, J. (1974). Tilt aftereffect following very brief exposures. *Vision Research*, *14*(1), 151–152. https://doi.org/10.1016/0042-6989(74)90133-3

Sillito, A. M. (1975). The effectiveness of bicuculine as antagonist of GABA and visually evoked inhibition in the cat's striate cortex. *Journal of Physiology*, *250*(2), 287–304. https://doi.org/10.1113/jphysiol.1975.sp011055

Sompolinsky, H., & Shapley, R. (1997). New perspectives on the mechanisms for orientation. *Current Opinion in Neurobiology*, *7*(4), 514–522. https://doi.org/10.1016/S0959-4388(97)80031-1

Song, Ch., Schwarzkopf, D. S., Lutti, A., Li, B., Kanai, R., & Rees, G. (2013). Effective connectivity within human primary visual cortex predicts interindividual diversity in illusory perception. *Journal of Neuroscience*, *33*(48), 18781–18791. https://doi.org/10.1523/JNEUROSCI.4201-12.2013

Storrs, K. R., & Arnold, D. H. (2015). Evidence for tilt normalization can be explained by anisotropic orientation sensitivity. *Journal of Vision*, *15*(1), 26, 1–11. http://dx.doi.org/10.1167/15.1.26

Sur, M., Schummers, J., & Dragoi, V. (2002). Cortical plasticity: Time for a change. *Current Biology*, *12*(5), R168–R170. https://doi.org/10.1016/S0960-9822(02)00733-9

Templeton, W. B., Howard, I. P., & Easting, G. (1965). Satiation and the tilt aftereffect. *American Journal of Psychology*, *78*(4), 656–659. http://dx.doi.org/10.2307/1420931

Vaitkevičius, H., Karalius, M., Meškauskas, A., Sinius, J., & Sokolov, E. (1983). A model for the monocular line orientation analyser. *Biological Cybernetics*, *48*(3), 139–147. https://doi.org/10.1007/BF00318081

Vaitkevičius, H., Viliunas, V., Bliumas, R., Stanikunas, R., Svegzda, A., Dzekeviciute, A., & Kulikowski, J. J. (2009). Influences of prolonged viewing of tilted lines on perceived line orientation: The normalization and tilt after-effect. *Journal of the Optical Society of America A*, *26*(7), 1553–1563. https://doi.org/10.1364/JOSAA.26.001553

Vidyasagar, T. (1985). Geniculate orientation biases as Cartesian coordinates for cortical orientation detectors. In D. Rose & V. G. Dobson (Eds.), *Models of the visual cortex* (pp. 390–395). New York: Wiley.

Wenderoth, P., & Zwan, R. V. (1989). The effects of exposure duration and surrounding frames on direct and indirect tilt aftereffects and illusions. *Perception and Psychophysics*, *46*(4), 338–344. https://doi.org/10.3758/BF03204987

Whitmire, C. J., & Stanley, G. B. (2016). Rapid sensory adaptation redux: A circuit perspective. *Neuron*, *92*(2), 298–315. https://doi.org/10.1016/j.neuron.2016.09.046

Wissig, S. C., & Kohn, A. (2012). The influence of surround suppression on adaptation effects in primary visual cortex. *Journal of Neurophysiology*, *107*(12), 3370–3384. http://dx.doi.org/10.1152/jn.00739.2011

Worgotter, F., & Koch, C. (1991). A detailed model of the primary visual pathway in the cat: Comparison of afferent excitatory and intracorbical inhibitory connecting schemes for orientation selectivity. *Journal of Neuroscience*, *11*(7), I959–1979. https://doi.org/10.1523/JNEUROSCI.11-07-01959.1991

Received April 24, 2019; accepted December 11, 2019.